

# The elusive Innermost Stable Circular Orbit: Now you see it, now you don't

Mariano Méndez

*SRON - Netherlands Institute for Space Research, Sorbonnelaan 2, 3584 CA Utrecht, The Netherlands*

*Astronomical Institute, University of Amsterdam, Kruislaan 403, 1098 SJ Amsterdam, The Netherlands*

**Abstract.** I study the behaviour of the maximum rms fractional amplitude,  $r_{\max}$  and the maximum coherence,  $Q_{\max}$ , of the kilohertz quasi-periodic oscillations (kHz QPOs) in a dozen low-mass X-ray binaries. I find that: (i) The maximum rms amplitudes of the lower and the upper kHz QPO,  $r_{\max}^{\ell}$  and  $r_{\max}^u$ , respectively, decrease more or less exponentially with increasing luminosity of the source; (ii) the maximum coherence of the lower kHz QPO,  $Q_{\max}^{\ell}$ , first increases and then decreases exponentially with luminosity; (iii) the maximum coherence of the upper kHz QPO,  $Q_{\max}^u$ , is more or less independent of luminosity; and (iv)  $r_{\max}$  and  $Q_{\max}$  show the opposite behaviour with hardness of the source, consistent with the fact that there is a general anticorrelation between luminosity and spectral hardness in these sources. Both  $r_{\max}$  and  $Q_{\max}$  in the sample of sources, and the rms amplitude and coherence of the kHz QPOs in individual sources show a similar behaviour with hardness. This similarity argues against the interpretation that the drop of coherence and rms amplitude of the lower kHz QPO at high QPO frequencies in individual sources is a signature of the innermost stable circular orbit around a neutron star.

**Keywords:** stars: neutron — X-rays: binaries

**PACS:** 95.85.Nv 97.60.Jd 97.80.Jp

## INTRODUCTION

Kilohertz quasi-periodic oscillations (kHz QPOs) in the X-ray flux of low-mass X-ray binaries have drawn much attention since their discovery, about ten years ago. The reason for this continued interest is that since they most likely reflect the motion of matter very close to the neutron star (or black hole), these QPOs may provide one of the few direct ways of measuring effects that are unique to the strong gravitational-field regime in these systems. Often two simultaneous kHz QPOs are seen in the power density spectra of low-mass X-ray binaries, the lower and the upper kHz QPO according to how they appear sorted in frequency.

Most of the work on QPOs in these years [see 1, for a review] has focused on the frequencies of these QPOs, because those frequencies provide insights into the dynamics of the system. For instance, different from the Newtonian theory of gravitation, in general relativity the effective potential as a function of radial distance to the central source has a maximum. A particle in a circular orbit at that radius would be in unstable equilibrium; if perturbed, the particle would fall onto the central object. This radius defines the innermost stable circular orbit, or ISCO. No stable orbit around the central object is possible inside the radius of the ISCO, which in the Schwarzschild case (non-rotating central object) is  $r_{\text{ISCO}} = 6GM/c^2$  [2]. If (at least) one of the QPOs

reflects Keplerian motion around the neutron star [3, 4], the ISCO would set a limit to the maximum frequency that the QPOs can reach [3]. By measuring that maximum frequency it would be possible to infer the mass and constrain the radius of the neutron star.

From the beginning there has been interest on the other two properties of the kHz QPOs, their amplitude and coherence [e.g., 5], but systematic studies of those other QPO properties only started to take off slightly later [e.g. 6–9].

Recently, Barret et al. [10–12] carried out a systematic study of the kHz QPO coherence and rms amplitude in three X-ray binaries, 4U 1636–53, 4U 1608–52, and 4U 1735–44. They find that in all three sources the coherence and rms amplitude of the lower kHz QPO increase slowly with frequency, and after the coherence and rms amplitude reach their maximum values, they decrease abruptly as the QPO frequency keeps on increasing. (The sudden drop is most noticeable in the coherence of the lower kHz QPO; in the case of the rms amplitude the drop is less abrupt.) Barret et al. propose that this behaviour is due to effects related to the ISCO around the neutron star in these systems.

Triggered by these results, I investigated the dependence of the maximum coherence and rms amplitude of both kHz QPOs in a large sample of low-mass X-ray binaries.

## DATA SELECTION AND ANALYSIS

All the data that I use here were obtained over the last 10 years with the Proportional Counting Array (PCA) on board the Rossi X-ray Timing Explorer (RXTE). I collected most of these data from the literature. For this I searched, for as many sources as possible, all published values of the rms fractional amplitude and the coherence of the kHz QPOs. [see 13, for a detailed description of the selection and characteristics of the data.] The coherence  $Q$  of a QPO is defined as  $Q = \nu_{\text{QPO}}/\lambda$ , where  $\nu_{\text{QPO}}$  and  $\lambda$  are the frequency and the full-width at half-maximum of the QPO. The rms amplitude,  $r$ , is calculated from  $P$ , the integral from 0 to  $\infty$  of the Fourier power under the QPO, and the source intensity,  $S$ , as  $r = 100 \times \sqrt{P/S}$ ; from this definition,  $r$  is expressed as a percent of the total intensity of the source.

Here I use the naming convention of [14], in which the lower kHz QPO is called  $L_\ell$ , and the upper kHz QPO is called  $L_u$ . The frequency, coherence and amplitude of each QPO carry a subscript or superscript  $\ell$  or  $u$ , respectively. I use the expression “kilohertz QPO” to refer to features in the power spectra of neutron star systems that have frequencies  $> 150$  Hz, and that have not been identified as hectohertz QPO [e.g., 8].

Once I have collected all  $Q_{\text{max}}$  and  $r_{\text{max}}$  values for each QPO for each source, and the frequencies  $\nu_\ell$  and  $\nu_u$  at which those maximum values occur, I use Figure 1 in [15] to get the corresponding source luminosity: Using the QPO frequency as input, I read off the luminosity of the source at that frequency from that Figure. For three sources, 4U 1608–52, 4U 1636–53, and 4U 1820–30, the maximum rms amplitudes of  $L_u$  occur in states of the source in which the QPO frequencies are outside the range of frequencies in Figure 1 of [15]. In those three cases I either search the literature for flux measurements of the source in that state, or I extract spectra from the corresponding *RXTE* observations, and

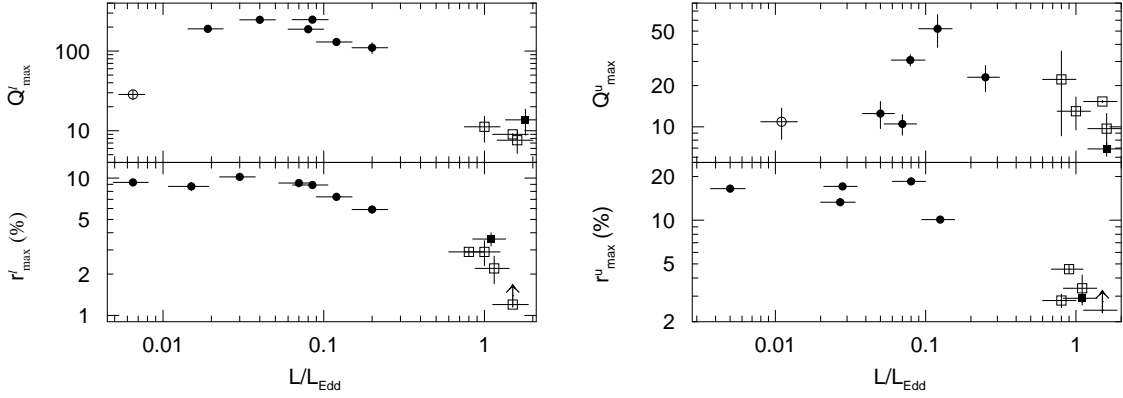


**FIGURE 1.** *Left panel:* The maximum coherence (upper panel) and maximum rms amplitude (lower panel) of the lower kHz QPO as a function of the source luminosity at the time at which those maximum values were reached. The luminosity is in units of the Eddington luminosity for a  $1.9M_{\odot}$  neutron star. Filled symbols indicate measurements over the full energy band covered by the PCA on board *RXTE*. Open circles indicate measurements over a limited energy band; in these cases (except for Sco X-1), the rms amplitudes have been divided by 1.25 [see 13, for details]. The rms amplitude in the case of Sco X-1 is not corrected for dead-time, and hence is only a lower limit (indicated with an arrow pointing upwards in the lower panel). Circles are Atoll sources; squares are Z sources. *Right panel:* The maximum coherence (upper panel) and maximum rms amplitude (lower panel) of the upper kHz QPO as a function of the source luminosity at the time at which those maximum values were reached. The luminosity is in units of the Eddington luminosity for a  $1.9M_{\odot}$  neutron star. Symbols are the same as in the left panel.

calculate the luminosities myself, or both.

The luminosities used here are uncertain for the following reasons: (i) Statistical error in the fluxes derived from model fitting. These errors are usually less than 5 – 10%. (ii) Accuracy in the determination of the luminosity for a given QPO frequency using the results of [15]. The reason for this is the so-called parallel-track phenomenon [e.g., 16], which introduces an uncertainty of the order of 20 – 50% in the luminosity [9]. (iii) The use of the 2 – 50 keV flux as a measure of the bolometric flux of the source. This effect contributes uncertainties of the order of 20 – 25% [see 15]. (iv) Uncertainty in the distance to these sources [see 15, for a discussion in the context of these sources]; this can yield uncertainties of up to 60% in the luminosity [see, e.g., 17]. In this paper I use a fixed error of 25% in the values of  $L/L_{\text{Edd}}$  as indicative of the error in the luminosity. It is clear from the previous discussion that this is a lower limit to the real error in this quantity.

## RESULTS

Figure 1 shows the dependence of the maximum coherence and maximum rms amplitude of both kHz QPOs as a function of source luminosity (in units of the Eddington luminosity for a  $1.9M_{\odot}$  neutron star). From this Figure it is apparent that  $r^u_{\text{max}}$  and  $r^l_{\text{max}}$  both decrease more or less exponentially with  $L/L_{\text{Edd}}$ . Using roughly the same sample of sources, [18] had already noticed that the rms amplitude of the upper kHz QPO decreases as the luminosity of the source increases.

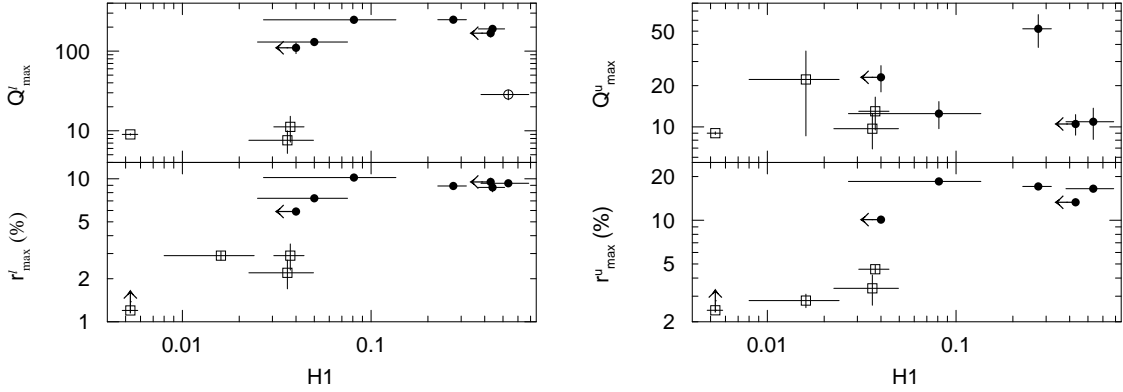


**FIGURE 2.** The maximum coherence (upper panels) and maximum rms amplitude (lower panels) of the lower kHz QPO (left) and the upper kHz QPO (right) as a function of the average source hardness,  $H1$ , defined as the ratio of the 40 – 80 keV to the 13 – 25 keV count rate, measured with *HEAO-1* [25, 26]. For an explanation of the symbols see the caption of Figure 1. The rms amplitudes in the case of Sco X-1 are not corrected for dead-time, and hence are lower limits (indicated with a vertical arrow in the lower panels). Upper limits to the hardness are indicated with horizontal arrows pointing to the left. I do not include GX 5-1 in this Figure because the *HEAO-1* measurements of this source suffer contamination from a previously unknown hard X-ray source in the field [see explanation in 26].

From the same Figure, it is also apparent that at low luminosity,  $Q_{\max}^{\ell}$  first increases with  $L$  up to  $L/L_{\text{Edd}} \sim 0.04$ , and then it decreases exponentially. On the other hand,  $Q_{\max}^u$  does not show any significant trend with luminosity.

The gap in Figure 1 at  $L/L_{\text{Edd}} \sim 0.25 - 0.7$  separates the Atoll sources at low  $L$ , and the Z sources at high  $L$  [see 19, for a definition of Atoll and Z sources]. That gap would be occupied by the four intermediate-type sources, GX 9+1, GX 9+9, GX 3+1, and GX 13+1, which so far have not shown any kHz QPOs [20–23]. The upper limit to the rms amplitude of the QPO in these sources ranges from 1.6% to 2.6%. Since the range of luminosities spanned by these sources [17] is  $L/L_{\text{Edd}} \sim 0.12 - 0.44$ , these upper limits are much lower than would be expected from the interpolation of the trends of  $r_{\max}^{\ell}$  and  $r_{\max}^u$  with  $L/L_{\text{Edd}}$  in Figure 1.

From Figure 1 it is apparent that the maximum rms amplitude of both kHz QPOs and the maximum coherence of the lower kHz QPO are consistently lower in the Z sources than in the Atoll sources (see also below). Since the detection of QPOs in Z sources generally require calculating average power spectra over longer time intervals than for Atoll sources, this difference could in principle be due to the frequency drift of the QPOs, which would artificially reduce their  $Q$  values. However, measurements of the coherence of the lower kHz QPO in the Atoll source 4U 1608–52 and the Z source Sco X-1 on short time intervals (less than a few hundred seconds), when  $\nu_{\ell} \sim 600$  Hz, yields  $Q_{\ell} = 74.0 \pm 4.6$  for 4U 1608–52, and  $Q_{\ell} = 4.2 \pm 0.4$  for Sco X-1. This shows that in the Z source Sco X-1, even over very short time intervals, the lower kHz QPO is intrinsically significantly broader than in the Atoll source 4U 1608–52.

From Figure 1 [see also 13] it is also apparent that, except for the case of 4U 0614+09,  $Q_{\max}^{\ell}$  and  $r_{\max}^{\ell}$  are positively correlated with each other. Concerning 4U 0614+09, the hardest source in the sample and the one at the lowest luminosity, it is as if in this case  $Q_{\max}^{\ell}$  were too low for  $r_{\max}^{\ell}$ , or conversely, as if  $r_{\max}^{\ell}$  were too high for  $Q_{\max}^{\ell}$ . Recent

work [24] confirms that the decrease of  $Q_{\max}^{\ell}$  at low luminosity is real.

Van Paradijs and van der Klis [25] have shown that there is a general correlation between the average source luminosity and the average source hardness, H1, defined as the ratio of the count rate in the 40 – 80 keV band to the count rate in the 13 – 25 keV band, measured with *HEAO-1* [see 26]. In that respect, as expected, the plots of  $Q_{\max}$  and  $r_{\max}$  vs. hardness in Figure 2 show that  $r_{\max}^u$  and  $r_{\max}^{\ell}$  both increase with the hardness ratio H1,  $Q_{\max}^{\ell}$  increases with H1 and then it decreases for 4U 0614+09, the hardest source in this sample, and as in the plots as a function of luminosity,  $Q_{\max}^u$  is consistent with being constant with H1. I caution the reader that contrary to the  $L/L_{\text{Edd}}$  values that I plot in Figure 1, for this Figure I use average values of the spectral hardness measured several years before the kHz QPOs were discovered. Notice that GX 340+0, for which the distance, and hence the luminosity, is uncertain, appears in Figure 2 close to the other Z sources (open symbols; GX 340+0 is the point at H1 = 0.036, just to the left of GX 17+2 at H1 = 0.037); since H1 is a distance-independent parameter, this suggests that the distance to GX 340+0 is not too much in error.

It is interesting to notice in this Figure that there is no gap in the distribution of sources as a function of hardness between the Z and Atoll sources. This is opposite to what is apparent in the plot of QPO parameters vs. luminosity, where there is a gap corresponding to the intermediate-type, the GX-sources (see above). The H1 values of the GX-sources range from 0.03 to 0.14.

Both in Figure 1 and 2 there appears to be a gap in the values of  $Q_{\max}^{\ell}$ , and perhaps also  $r_{\max}^{\ell}$  and  $r_{\max}^u$  between the Z and Atoll sources. I have just shown that this difference is real, and is not an artifact due to the way the QPOs are measured. While this difference may indicate a dependence on luminosity (see Fig. 1) or on spectral hardness (see Fig. 2), this could also point to a difference between Z and atoll sources. It is worth noting, however, that there is still a trend of  $Q_{\max}^{\ell}$  and both rms amplitudes *within* the atoll sources in Figure 1. Furthermore, there is a significant trend in the relations between  $Q_{\max}$  and  $r_{\max}$  within the atoll sources; e.g., the relation between  $Q_{\max}^{\ell}$  and  $r_{\max}^{\ell}$  is  $8\sigma$  different from a constant [see 13, for details]. All this suggests that the distinction between Z and Atoll sources cannot be the (only) explanation for this difference.

## DISCUSSION

I study the maximum amplitude,  $r_{\max}$ , and maximum coherence,  $Q_{\max}$ , of the kHz QPOs as a function of luminosity and hardness for a large sample of low-mass X-ray binaries. I show that the maximum coherence of the lower kHz QPO,  $Q_{\max}^{\ell}$ , first increases up to  $L \sim 0.04L_{\text{Edd}}$  and then decreases with luminosity, whereas the maximum coherence of the upper kHz QPO,  $Q_{\max}^u$ , is independent of luminosity. I also find that the maximum rms amplitudes of both the lower and the upper kHz QPOs,  $r_{\max}^{\ell}$  and  $r_{\max}^u$ , respectively, decrease monotonically with luminosity and increase monotonically with the hardness of the source. [The dependence of  $r_{\max}^u$  on luminosity and hardness was first reported by 18].

From the above results it follows that for all sources,  $r_{\max}^{\ell}$  and  $r_{\max}^u$  are positively correlated with each other. Also, for all sources with  $L \gtrsim 0.04L_{\text{Edd}}$ , that is all sources in this paper except 4U 0614+09, the hardest source in the sample and the one at the lowest

luminosity,  $Q_{\max}^{\ell}$  is positively correlated both with  $r_{\max}^{\ell}$  and  $r_{\max}^u$ .  $Q_{\max}^u$  is independent of  $Q_{\max}^{\ell}$  or the maximum rms amplitude of the kHz QPOs.

In individual sources, both  $r_{\ell}$  and  $Q_{\ell}$  increase with  $v_{\ell}$  and then drop rather abruptly at the high end of the  $v_{\ell}$  range;  $r_u$  also increases and then drops at high  $v_u$  values, and  $Q_u$  is more or less constant or increases slightly with  $v_u$  [e.g., 7, 9, 27]. In the case of 4U 1636–53, [11] interpret the sudden drop of the coherence and rms amplitude of  $L_{\ell}$ , together with the existence of a frequency above which  $L_{\ell}$  is not detected, as evidence of the innermost stable circular orbit around the neutron star in this system.

From the results of individual sources and those of the sample of sources that I present in this paper, it is apparent that the behaviour of the coherence and rms amplitude of the kHz QPOs as a function of the *QPO frequency* in *individual sources* is similar to the behaviour of the maximum coherence and maximum rms amplitude of the kHz QPOs as a function of *luminosity* in the *sample of sources*. Since in individual sources there is a general relation between QPO frequencies and source intensity, in the sense that at higher intensity the QPOs generally appear at higher frequencies (but remember the parallel-track effect), this raises the question of whether the same mechanism may be behind both behaviours.

The link between these two behaviours need not be luminosity, but could be the high-energy emission (or hardness) in these systems. On one hand, in the sample of sources the maximum coherence and maximum rms amplitude of the kHz QPO, except the maximum rms amplitude of  $L_u$ , appear to correlate fairly well with spectral hardness (see Figure 2), while on the other hand in individual sources the QPO frequencies are well correlated with the spectral hardness of the source [16], the index of the power law that fits the high-energy part of the X-ray spectrum [28], or  $S$ , a parameter that measures the position along the track traced out by the source in a colour-colour or colour-intensity diagram [called  $S_z$  and  $S_a$  in the Z and Atoll sources, respectively; see e.g., 6, 29]. From this, it follows that in individual sources there should be a relation between QPO rms amplitude and coherence on one hand and spectral hardness on the other.

The comparison between individual sources and the sample of sources suggests that the same mechanism is responsible for the drop of coherence and rms amplitude of the lower kHz QPO with QPO frequency in individual sources as well as for the drop of maximum QPO coherence and maximum QPO rms amplitude with luminosity in the sample of sources. Most likely the mechanism is related to the high-energy emission in these systems. This does not necessarily mean that the fractional emission at high energies (represented by the hardness or X-ray colours) is the root mechanism that drives all QPO parameters (QPO frequency, coherence, and rms amplitude). For instance, one possibility (there could be many others) is that the (instantaneous) mass accretion rate sets the size of the inner radius of the disc [30], which in turn determines the QPO frequency as well as the relative contribution of the high-energy part of the spectrum to the total luminosity. If the efficiency of the modulation mechanism (related to the rms amplitude  $r$ ) and the lifetime of the oscillations (related to the coherence  $Q$ ) that produce the QPO depended upon the emission from the high-energy part of the source spectrum [see 13, for a discussion of possible ways in which this could happen], observationally it would appear as if the coherence and rms amplitude of the QPO depended upon the QPO frequency, and hence upon the radius in the disc at which the QPO is produced. The

sudden drop of the coherence and rms amplitude of the QPO at some QPO frequency would then appear to be associated to a dynamical peculiarity in the accretion disc, for instance the ISCO. Observing the same source repeatedly would not allow to distinguish the above scenario from one in which QPO coherence and rms amplitude were actually set by QPO frequency or the dynamics in the accretion disc.

To distinguish between these two options, one would need to observe a sample of sources of kHz QPOs for which the mass-accretion rate, and hence the relative contribution of the high-energy part of the spectrum to the total emission, was different from source to source. In that case, QPO coherence and rms amplitude would drop for sources accreting mass at higher rates, even if the frequency of the QPO was more or less the same from source to source. Since, as I have shown in this paper, this is the general behaviour observed in sources of kHz QPOs, it is reasonable to infer that a mechanism similar to the one I described in the previous paragraph is effective in setting the coherence and rms amplitude of the kHz QPOs. If this is correct, this also implies that the drop of QPO coherence and rms amplitude as a function of QPO frequency in individual sources cannot be due to effects of the ISCO.

Note also that in individual sources not just the rms amplitude of the kHz QPOs, but also the rms amplitude of other lower-frequency QPOs decrease with increasing QPO frequency. For instance, in four Atoll sources, 4U 1728–34, 4U 1608–52, 4U 0614+09, and 4U 1636–53, the rms amplitudes of the “bump”, a QPO at  $\sim 0.1 - 30$  Hz, the “hump”, a QPO at  $\sim 1 - 40$ , and the hectohertz QPO at  $\sim 100 - 300$  Hz, all drop as the frequencies of the kHz QPOs increase, in a similar fashion as the amplitude of the upper and lower kHz QPOs [e.g., 31, and references therein; see also there a description of these other QPOs]. This also argues against the interpretation of the ISCO as the cause of the drop of the rms of the kHz QPOs, and indicates that the amplitudes of *all* variability components are set by the same mechanism which, as I suggested, could be the same one that governs the high-energy spectral component.

## CONCLUSION

I study the maximum amplitude,  $r_{\max}$ , and maximum coherence,  $Q_{\max}$ , of the kHz QPOs as a function of luminosity and hardness for a dozen low-mass X-ray binaries. I find that: (i) The maximum coherence of the lower kHz QPO,  $Q_{\max}^{\ell}$ , first increases up to  $L \sim 0.04L_{\text{Edd}}$  and then decreases with luminosity. (ii) The maximum coherence of the upper kHz QPO,  $Q_{\max}^{\text{u}}$ , is independent of luminosity. (iii) The maximum rms amplitudes of both the lower and the upper kHz QPOs,  $r_{\max}^{\ell}$  and  $r_{\max}^{\text{u}}$ , respectively, decrease monotonically with luminosity. (iv) Both  $r_{\max}^{\text{u}}$  and  $r_{\max}^{\ell}$  increase with the source hardness,  $Q_{\max}^{\ell}$  first increases with hardness and then drops for the hardest source in the sample, and  $Q_{\max}^{\text{u}}$  is independent of hardness. (v) The relation between  $Q_{\max}$  and  $r_{\max}$  with luminosity in the sample of sources is similar to the relation between  $Q$  and  $r$  with QPO frequency in individual sources. (vi) The above argues against the interpretation that the drop of QPO coherence and QPO rms amplitude at high QPO frequency in individual sources is due to effects related to the innermost stable orbit around the neutron star in these systems.

## ACKNOWLEDGMENTS

I thank Didier Barret and Cole Miller for valuable discussions on the ideas that I present in this paper. I am grateful to Manuel Méndez for his collaboration, and to Ahmed and Lidy Helmi for their hospitality during the period in which I did this work. This research has made use of data obtained through the High Energy Astrophysics Science Archive Research Center Online Service, provided by the NASA/Goddard Space Flight Center. The Netherlands Institute for Space Research (SRON) is supported financially by NWO, the Netherlands Organisation for Scientific Research.

## REFERENCES

1. van der Klis, M. 2006, in *Compact stellar X-ray sources*, ed. W. H. G. Lewin, and M. van der Klis (Cambridge: Cambridge Univ. Press), 39.
2. Bardeen, J. M., Press, W. H., and Teukolsky, S. A. 1972, *ApJ*, 178, 347.
3. Miller, M. C., Lamb, F. K., and Psaltis, D. 1998, *ApJ*, 508, 791
4. Stella, L., and Vietri, M. 1999, *Phys. Rev. Lett.*, 82, 17
5. van der Klis, M., Wijnands, R., Horne, K., and Chen, W. 1997, *ApJ*, 481, L97
6. Jonker, P. G., et al. 2000, *ApJ*, 537, 374
7. Di Salvo, T., Méndez M., van der Klis, M., Ford, E. C., and Robba, N. R. 2001, *ApJ*, 546, 1107
8. van Straaten, S., Ford, E. C., van der Klis, M., Méndez M., and Kaaret, P. 2000, *ApJ*, 540, 1049
9. Méndez, M., van der Klis, M., and Ford, E. C. 2001, *ApJ*, 561, 1016
10. Barret, D., Kluźniak, W., Olive, J. F., Paltani, S., and Skinner, G. K. 2005a, *MNRAS*, 357, 1288
11. Barret, D., Olive, J. F., and Miller, M. C. 2005b, *MNRAS*, 361, 855
12. Barret, D., Olive, J. F., and Miller, M. C. 2005c, *AN*, 326, 808
13. Méndez, M. 2006, *MNRAS*, 371, 1925
14. Belloni, T., Psaltis, D., and van der Klis, M. 2002, *ApJ*, 572, 392
15. Ford, E. C., van der Klis, M., Méndez, M., Wijnands, R., Homan, J., Jonker, P. G., and van Paradijs, J. 2000, *ApJ*, 537, 368
16. Méndez, M., van der Klis, M., Ford, E. C., Wijnands, R., and van Paradijs, J. 1999, *ApJ*, 511, L49
17. Christian, D. J. and Swank, J. H. 1997, *ApJS*, 109, 177
18. Jonker, P. G., et al. 2001, *ApJ*, 553, 335
19. Hasinger, G., and van der Klis, M. 1989, *A&A*, 225, 79
20. Strohmayer, T. E. 1998, in *AIP Conf. Proc.* 431, *Accretion Processes in Astrophysical Systems: Some Like it Hot!*, ed. Stephen S. Holt and Timothy R. Kallman (New York: AIP), 397
21. Wijnands, R., van der Klis, M., and van Paradijs, J. 1998c, *IAU Symp.* 188, *The Hot Universe*, K. Koyama et al. (eds.), 370
22. Homan, J., van der Klis, M., Wijnands, R., Vaughan, B., and Kuulkers, E. 1998, *ApJ*, 499, L41
23. Oosterbroek, T., Barret, D., Guainazzi, M., and Ford, E. C. 2001, *A&A*, 366, 138
24. Barret, D., Olive, J. F., and Miller, M. C. 2006, *MNRAS*, 370, 1140.
25. van Paradijs, J., and van der Klis, M. 1994, *A&A*, 281, L17
26. Levine, A. M., et al. 1984, *ApJS*, 54, 581
27. Di Salvo, T., Méndez, M., and van der Klis, M. 2003, *A&A*, 406, 177
28. Kaaret, P., Yu, W., Ford, E. C., and Zhang, N. S. 1998, *ApJ*, 497, L93
29. Méndez, M., and van der Klis, M. 1999, *ApJ*, 517, L51
30. van der Klis, M. 2001, *ApJ*, 561, 943
31. Altamirano, D., et al. 2006, *ApJ*, submitted